

University of Nebraska - Lincoln

DigitalCommons@University of Nebraska - Lincoln

---

Faculty Publications from the Department of  
Electrical and Computer Engineering

Electrical & Computer Engineering, Department of

---

9-7-2006

# Optical emission in magnetically confined laser-induced breakdown spectroscopy

X. K. Shen

*University of Nebraska - Lincoln*

Yongfeng Lu

*University of Nebraska - Lincoln, ylu2@unl.edu*

T. Gebre

*University of Nebraska - Lincoln*

Hao Ling

*University of Nebraska - Lincoln, hling4@unl.edu*

Y. X. Han

*University of Nebraska - Lincoln*

Follow this and additional works at: <http://digitalcommons.unl.edu/electricalengineeringfacpub>



Part of the [Electrical and Computer Engineering Commons](#)

---

Shen, X. K.; Lu, Yongfeng; Gebre, T.; Ling, Hao; and Han, Y. X., "Optical emission in magnetically confined laser-induced breakdown spectroscopy" (2006). *Faculty Publications from the Department of Electrical and Computer Engineering*. 90.  
<http://digitalcommons.unl.edu/electricalengineeringfacpub/90>

This Article is brought to you for free and open access by the Electrical & Computer Engineering, Department of at DigitalCommons@University of Nebraska - Lincoln. It has been accepted for inclusion in Faculty Publications from the Department of Electrical and Computer Engineering by an authorized administrator of DigitalCommons@University of Nebraska - Lincoln.

# Optical emission in magnetically confined laser-induced breakdown spectroscopy

X. K. Shen, Y. F. Lu,<sup>a)</sup> T. Gebre, H. Ling, and Y. X. Han

*Department of Electrical Engineering, University of Nebraska-Lincoln, Lincoln, Nebraska 68588-0511*

(Received 2 February 2006; accepted 15 June 2006; published online 8 September 2006)

Magnetically confined laser-induced breakdown spectroscopy was investigated by studying the optical emission from laser-induced plasma plumes expanding across an external transverse magnetic field. KrF excimer laser pulses with a pulse duration of 23 ns and a wavelength of 248 nm were used to produce plasmas from Al, Cu, and Co targets. Various optical emission lines obtained from Al and Cu targets show an obvious enhancement in the intensity of optical emission when a magnetic field of  $\sim 0.8$  T is applied, while the optical emission lines from Co targets show a decrease in the optical emission intensity. The enhancement factors of optical emission lines were measured to be around 2 for the Al and Mn (impurity) lines from Al targets, and 6–8 for Cu lines from Cu targets. Temporal evolution of the optical emission lines from the Al samples shows a maximum enhancement in emission intensity at time delays of 8–20  $\mu$ s after the incident laser pulse, while from the Cu targets it shows a continuous enhancement at time delays of 3–20  $\mu$ s after the pulse. The enhancement in the optical emission from the Al and Cu plasmas was presumably due to the increase in the effective plasma density as a result of magnetic confinement. The decrease in the emission intensity from the Co plasmas was suggested to be due to the decrease of effective plasma density as a result of the magnetic force. © 2006 American Institute of Physics.

[DOI: [10.1063/1.2337169](https://doi.org/10.1063/1.2337169)]

## I. INTRODUCTION

Laser-induced breakdown spectroscopy (LIBS) is a useful diagnostic tool by studying the atomic and ionic emission spectroscopies from laser-induced plasmas.<sup>1</sup> Laser-induced breakdown is the generation of a luminous and ionized gas (plasma) by focusing a high-intensity laser to various gas, liquid, or solid samples. LIBS has certain advantages such as the simplicity of the method, the ability to simultaneously monitor all elements in the plasma, the nonrequirement of sample preparation, and the ability to analyze samples in air. LIBS is considered as a suitable tool for real-time monitoring of radioactive material in the nuclear (waste) industry.<sup>2</sup> Recently, LIBS has been used successfully in the analysis of trace elements and in the detection of radioactive elements, and it has also been used in hair tissue mineral analysis.<sup>3,4</sup>

The detection sensitivity of LIBS varies significantly between the different elements and is dependent on the element and excitation properties of sample sources. Some techniques have been developed to improve the LIBS sensitivity, such as oblique incidence of laser upon the surface<sup>5</sup> and dual-pulse excitation.<sup>6,7</sup> In recent years, the use of a magnetic field to confine laser-induced plasmas has attracted more and more interest. The magnetic field can be employed to better control the dynamic properties of the transient and energetic plasmas. The presence of a magnetic field during the expansion of laser-induced plasmas may initiate several

interesting phenomena, including conversion of the plasma kinetic energy into thermal energy, plume confinement, ion acceleration, emission enhancement, plasma instabilities, and other phenomena.<sup>8</sup>

The interaction of an expanding plasma with a magnetic field has been studied by many groups. Bhadra postulated that laser-induced plasmas would be stopped by a magnetic field  $B$  in a distance  $R \sim B^{-2/3}$ .<sup>9</sup> Dimonte and Wiley studied that the magnetic containment radius is on the order of  $R_b = (3E_k \mu_0 / 2\pi B_0^2)^{1/3}$  in mks units, where  $\mu_0$  is the free-space permeability,  $B_0$  is the magnetic field, and  $E_k$  is the plasma kinetic energy.<sup>10</sup> Neogi and Thareja investigated the dynamics of laser-produced carbon plasmas expanding in a nonuniform magnetic field by emission spectroscopy and fast photography. They reported that oscillations in the temporal evolution of emission species were observed, which they attributed to edge instability. They also observed a double-peak structure in the temporal profile of C II and C III transitions.<sup>11,12</sup>

In this work, we studied the enhancement of optical emission in LIBS due to the magnetic confinement of laser-ablated plasmas. The effects of transverse magnetic field on the intensities of the LIBS spectra of the aluminum alloy, copper, and cobalt targets were investigated. The optical emissions were detected at the brightest points of the plasmas. The temporal evolutions of the optical emissions were studied to better understand the dynamics and magnetic confinement of the laser-ablated plasmas in LIBS. The fast imaging of the plasma plumes was also studied using a Nikon macrolens and an intensified charge-coupled device (CCD).

<sup>a)</sup> Author to whom correspondence should be addressed; electronic mail: ylu2@unl.edu

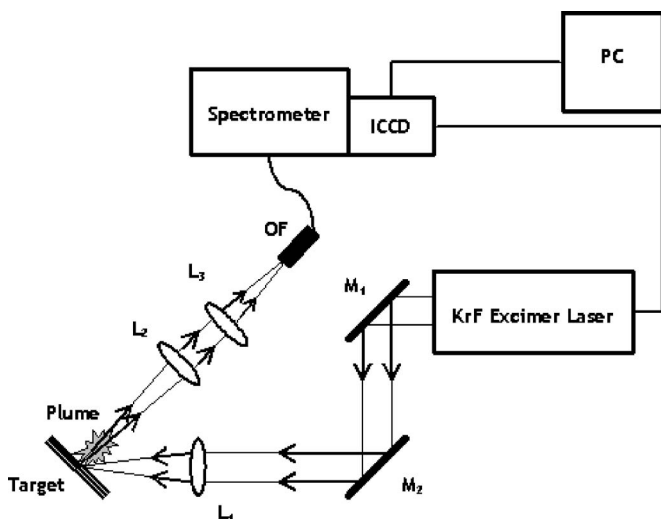


FIG. 1. Schematic diagram of the experimental setup for laser-induced breakdown spectroscopy.

## II. EXPERIMENTAL SETUP

The experimental setup used in this study is shown in Fig. 1. A KrF excimer laser (Lambda Physik, Compex 205, wavelength of 248 nm, pulse duration of 23 ns) that can deliver a pulse energy of 100–600 mJ was used in the experiment. For synchronization, the laser was operated at the external trigger mode. The laser was focused onto a target at an incident angle of  $45^\circ$  by an UV-grade quartz lens ( $L_1$ ) of 17 cm focal length. The sample target was placed in air. The optical emission from the laser-induced plasmas was coupled to an optical fiber by a pair of UV-grade quartz lenses ( $L_2$ : 5 cm focal length,  $L_3$ : 15 cm focal length). The plume size is around several millimeters and we only studied the optical emissions at the center position of the plasma where the continuum background emission is the strongest. The optical fiber has a  $50\ \mu\text{m}$  core diameter, with its exit end coupled to an optical spectrograph (Andor Tech., ME 5000). The wavelength range of this spectrograph is 200–950 nm with a spectral resolution of  $\lambda/\Delta\lambda=5000$ . A  $1024 \times 1024$  pixel intensified charge-coupled device (ICCD) (Andor Tech., iStar DH-734) was attached to the exit focal plane of the spectrograph and used to detect the optical emissions from the laser-induced plasmas. The ICCD detector was operated in the gated mode and it sent a trigger signal to the pulsed excimer laser. Data acquisition and analysis were performed with a personal computer (PC). The gate delay time and the gate width were adjusted to maximize the signal-to-background and signal-to-noise ratios. Five spectra corresponding to five laser pulses were accumulated to produce one spectrum and five such spectra were recorded for every condition to increase the sensitivity of the system and reduce the standard deviation. For the fast photography measurements, a Nikon macrolens (105 mm  $f/2.8D$ ) was attached to the Andor ICCD. The images were taken from the side of the plasmas.

Two permanent magnets with a size of  $3 \times 1 \times 1\ \text{in.}^3$  were used to produce a steady magnetic field. The magnets were fixed in a plastic structure with a space of 0.5 in. in which a magnetic field of 0.8 T was produced. The magnetic

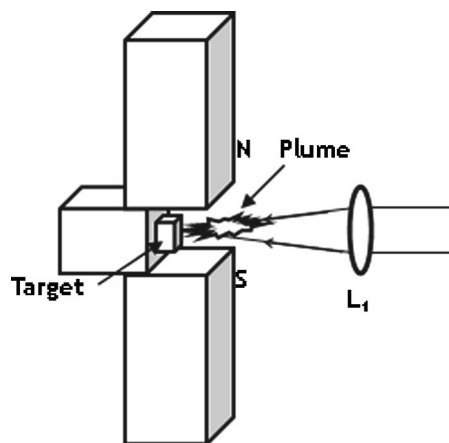


FIG. 2. Arrangement of the magnets and the location of the sample.

field was measured with a dc magnetometer. Samples were placed in the space in such a way that they have equal distances from both magnetic poles (Fig. 2). The laser beam was focused on the target surfaces so that the plasma plumes expanded in a nearly uniform magnetic field. The purity of the Cu target was 99.999%. The Al alloy target had a Mn impurity around 1%. The purity of the Co target was 99.95%.

## III. RESULTS AND DISCUSSION

The LIBS spectra of an Al alloy target were measured with and without the presence of a magnetic field. Figure 3 shows the Al and Mn spectral lines in the LIBS spectra with (solid curve) and without (dotted curve) the presence of the magnetic field (0.8 T) in a spectral range from 392 to 406 nm. The Al target was ablated by KrF excimer laser pulses with a laser fluence of  $7\ \text{J}/\text{cm}^2$ . The spectra were recorded by the gated ICCD camera with a gate delay of  $2\ \mu\text{s}$  and a gate width of  $20\ \mu\text{s}$ . The spectral lines of Al I (394.4 and 396.1 nm) and Mn I (403.1, 403.3, and 403.5 nm) were clearly observed. During this time period ( $2\text{--}20\ \mu\text{s}$ ), no apparent Al and Mn ionic emissions were observed. It is

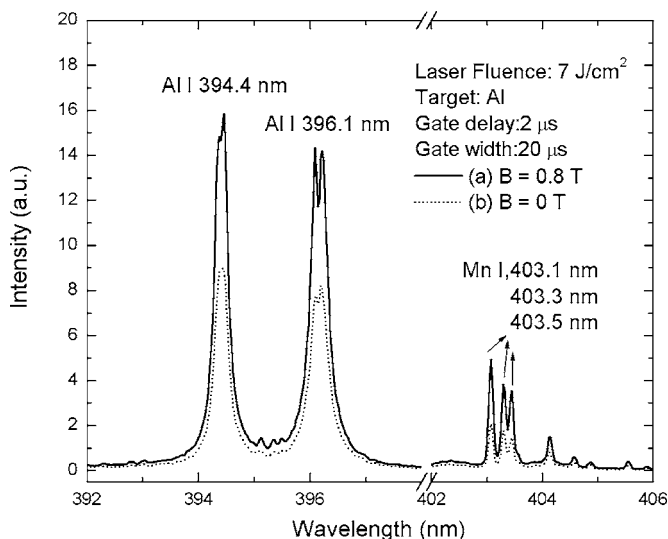


FIG. 3. Time integrated LIBS of an Al target at a gate delay of  $2\ \mu\text{s}$  and a gate width of  $20\ \mu\text{s}$ : (a) with (solid curve) and (b) without magnetic field (dotted curve).

clear that the atomic spectral lines for both Al and Mn were enhanced by a factor of 2 when a magnetic field of 0.8 T was introduced. This enhancement is probably attributed to the magnetic confinement of laser-induced plasmas. When an external magnetic field is applied to the laser-induced plasma, the electrons and ions in the plasma are influenced by the Lorentz force, and the expansion and diffusion of plasma are decelerated by the magnetic field. From magnetohydrodynamics (MHD) equations, the parameter  $\beta$  of plasma is given by

$$\beta \equiv \frac{8\pi nkT_e}{B^2} = \frac{\text{Particle pressure}}{\text{Magnetic field pressure}}. \quad (1)$$

The plasma parameter  $\beta$  is the ratio of particle pressure and magnetic field pressure, which indicates the size of the diamagnetic effect.<sup>13</sup> The deceleration of the plasma expansion under the influence of a magnetic field can be given as<sup>14</sup>

$$\frac{v_2}{v_1} = \left(1 - \frac{1}{\beta}\right)^{1/2}, \quad (2)$$

where  $v_1$  and  $v_2$  are, respectively, the asymptotic plasma expansion velocity in the absence and in the presence of the magnetic field. When  $\beta=1$ , the plasma would be stopped by the magnetic field. In the case of high  $\beta$ , the magnetic confinement would not be obvious. In the case of low  $\beta$  plasma, the magnetic confinement would be effective. Some oxygen and nitrogen atomic lines were also observed in the spectra at the gate delay from several hundred nanoseconds to 2  $\mu\text{s}$ . They vanished after the gate delay of 2  $\mu\text{s}$ . It shows that the air is ionized by the laser pulse and by the collision with the laser-induced Al plasmas. However, it is considered that there is no significant effect caused by the air plasma during the magnetic confinement of the laser-induced plasmas, since the density of the air plasmas is believed to be very low and their lifetime is around several microseconds. The plasma size was around 5 mm in diameter. The distance between the two permanent magnets was about 13 mm. Although the space between the magnets was much larger than the size of plasma, plasma-wall interaction might occur, which may also contribute to the confinement effect. Further study about plasma-wall interaction will be carried out in detailed research.

Since the laser-induced plasma is a pulsed source, the emission characteristics are a function of time. In order to better understand the dynamics of laser-induced plasmas and their optical emission, the temporal evolution of the optical emission lines from the plasmas were investigated by recording the spectra during distinct time intervals as the plasma decays. Figures 4 and 5 show the temporal evolution of the Al atomic line (394.4 nm) and Mn atomic line (403.1 nm) in the LIBS spectra as a function of gate delay with (solid curve) and without (dotted curve) the presence of a magnetic field of 0.8 T. Within the first few hundred nanoseconds after the laser pulse, the spectra are dominated by spectrally broad continuum due to the bremsstrahlung radiation and electron-ion recombination, which were not shown in the figures. The intensities of Al and Mn spectral lines were obtained by calculating the area of the lines; the first point was acquired

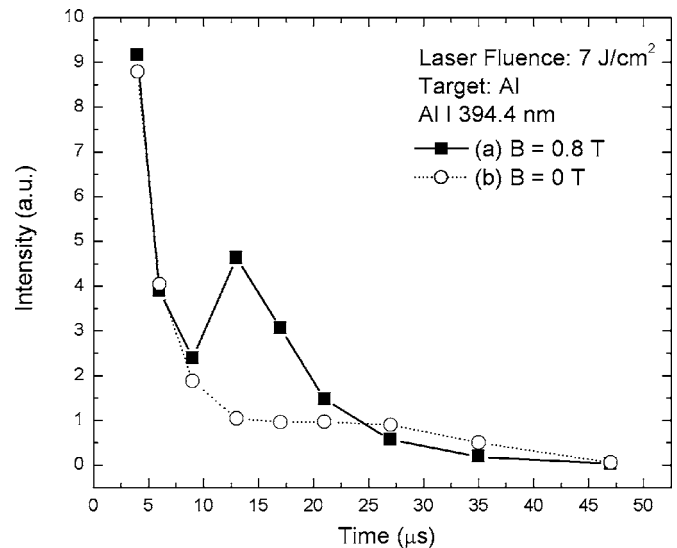


FIG. 4. Emission intensity evolution of Al spectral lines (394.4 nm, Al I): (a) with (solid curve) and (b) without magnetic field (dotted curve).

with a gate delay of 3  $\mu\text{s}$  and each point was acquired with a gate width of 2  $\mu\text{s}$ . As can be seen in Figs. 4 and 5 both of the Al and Mn atomic lines lasted for nearly 50  $\mu\text{s}$  regardless of the presence of the magnetic field. The emission intensity of the atomic line is proportional to the number density of the corresponding excited atoms and the transition probability. The transition probability is not considered to change much by the magnetic field (0.8 T), so the emission intensity is presumably related to the number density of the excited atoms. When there was no magnetic field, the emission lines decreased monotonously as the gate delay increased because the density of the excited atoms decreases due to the reduction of temperature and electron density as the plume expands and cools. It shows that the optical emission was enhanced by a magnetic field of 0.8 T as the gate delay increased from 8 to 20  $\mu\text{s}$ . The optical emission decreased gradually when the gate delay increased further from 20  $\mu\text{s}$ . A maximum enhancement factor of nearly 4.5 for Al spectral

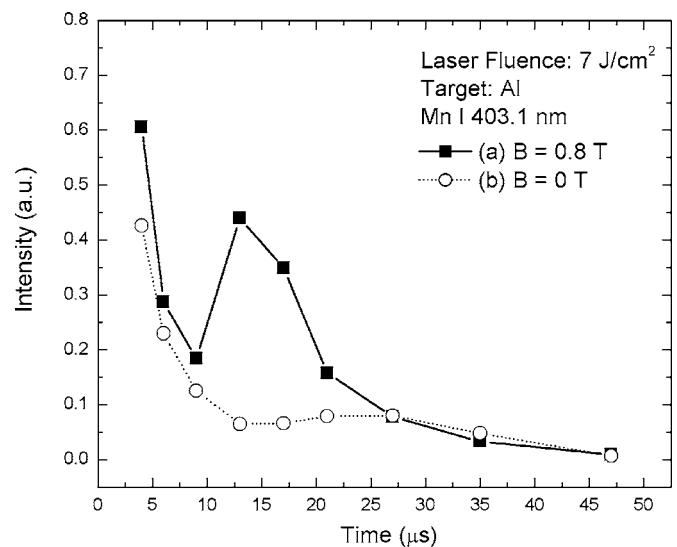


FIG. 5. Emission intensity evolution of Mn spectral lines (403.1 nm, Mn I): (a) with (solid curve) and (b) without magnetic field (dotted curve).

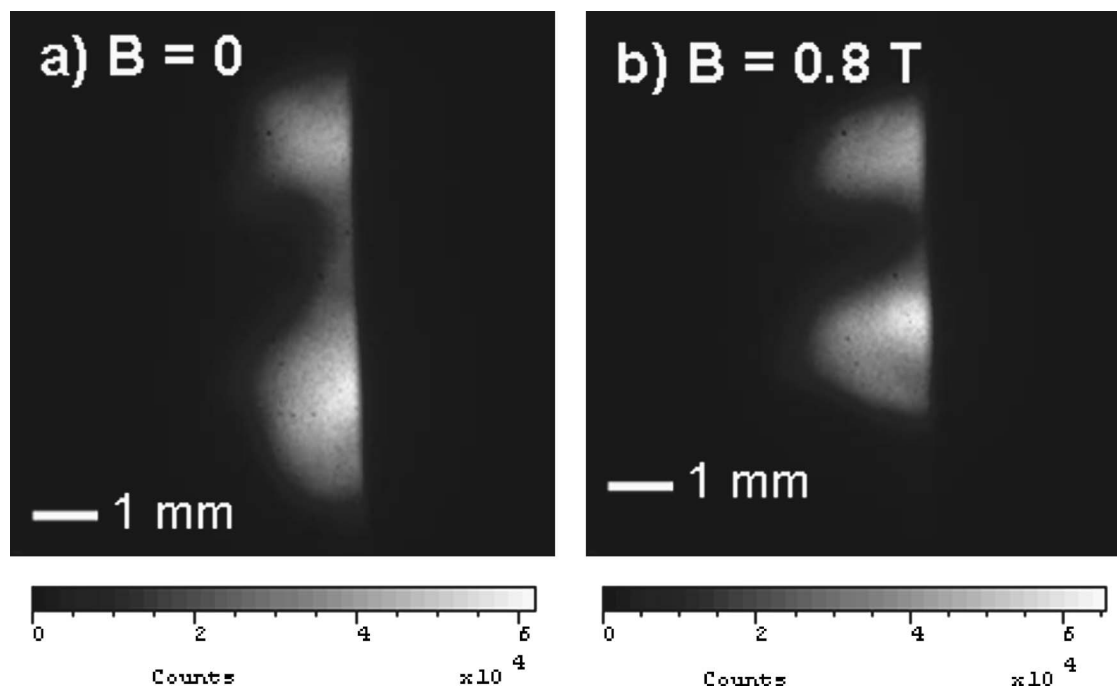


FIG. 6. Images of laser-induced Al plasmas with a gate delay of  $15 \mu\text{s}$  and a gate width of  $1 \mu\text{s}$ : (a) with and (b) without the presence of a magnetic field.

line is observed at a gate delay of  $13 \mu\text{s}$ . Various processes are responsible for the enhancement, including three-body recombination, radiative recombination, charge exchange, and magnetohydrodynamic instability.<sup>11</sup> Among them, radiative recombination is possibly the most dominant process. When the plasma expands and flies away from the target, the plasma temperature starts to decrease, and the possibility of recombination radiation ( $\propto 1/T^{3/2}$ ) rises. The density effect ( $\propto n_e n_i$ ) is also important. The enhancement in optical emission is probably due to the enhancement of the radiative recombination as a result of increased effective density due to magnetic confinement.<sup>15</sup>

Figure 6 shows the images of laser-induced Al plasmas with a gate width of  $1 \mu\text{s}$  at a gate delay of  $15 \mu\text{s}$  without [Fig. 6(a)] and with [Fig. 6(b)] the magnetic field (0.8 T). The Al target was ablated by KrF excimer laser pulses with a fluence of  $7 \text{ J/cm}^2$ . They are the side views of the plasmas. The plume size without the magnetic field is around 5 mm in length. Due to the presence of the air, the plasma plume was confined in a region of around 2 mm from the target surface both with and without the presence of the magnetic field at all the gate delay times. The plume gradually split into two parts after a gate delay of  $2 \mu\text{s}$ . With the presence of the magnetic field, the two parts were confined and were merged with each other gradually as the gate delay increased. It can be seen from Fig. 6 that the two parts with the presence of the magnetic field are closer to each other than those without magnetic field. We also took some images from the top of the plasma; the plasma plume gradually evolved into a shape like a toroid after a gate delay of  $2 \mu\text{s}$ .

The magnetic confinement of laser-ablated Al plasmas at different laser fluences were also investigated. Figure 7 shows the temporal evolution of the Al atomic line (394.4 nm) at several laser fluences. As can be seen in these graphs, the emission intensities were all enhanced in the

presence of a magnetic field of 0.8 T during a time period from 7 to around  $23 \mu\text{s}$ . As the laser fluence increases, the Al atomic line emissions are enhanced earlier and more obviously in the time period from 7 to around  $23 \mu\text{s}$ , and decay more rapidly further than  $23 \mu\text{s}$ . Figure 8 shows the variation of enhancement factor with gate delay at different laser fluences. It is assumed that at higher laser fluence the plasma is more energetic and more ionized so that the magnetic field can confine the plasma better; the plasma also cools down more rapidly due to the confinement, so the emission decreases more rapidly after a gate delay of  $23 \mu\text{s}$ .

We investigated the LIBS spectra of Cu targets at a laser fluence of  $7 \text{ J/cm}^2$ . Figure 9 shows the LIBS spectra of Cu recorded with (solid curve) and without (dotted curve) the magnetic field (0.8 T) in both spectral ranges of 320–330 and 510–525 nm. The spectra were recorded by the gated ICCD with a gate delay of  $9.3 \mu\text{s}$  and a gate width of  $10 \mu\text{s}$ . The spectral lines of atomic Cu at 515.3 and 521.8 nm were enhanced by a factor of 6–8 times when a magnetic field of 0.8 T was applied to confine the laser-ablated Cu plasmas. The reason for the enhancement is similar to the case of Al samples. Pant *et al.*<sup>16</sup> reported that an enhancement of two to three times in x-ray emission from copper plasma expanding across an externally applied magnetic field (0.6 T) has been observed for a laser intensity range of  $\sim 5 \times 10^{11}$ – $5 \times 10^{12} \text{ W/cm}^2$ .

Figure 10 shows the optical emission intensity for the Cu atomic line at 515.3 nm as a function of gate delay time with (solid curve) and without (dotted curve) the presence of a magnetic field (0.8 T). The first point was acquired with a gate delay of  $3 \mu\text{s}$  and each point was acquired with a gate width of  $3 \mu\text{s}$ . With the presence of a magnetic field, the optical emission increased as the gate delay increased from 3 to  $20 \mu\text{s}$ . The optical emission intensity lasted for nearly  $30 \mu\text{s}$ . Similar to the case of Al, the enhancement is due to



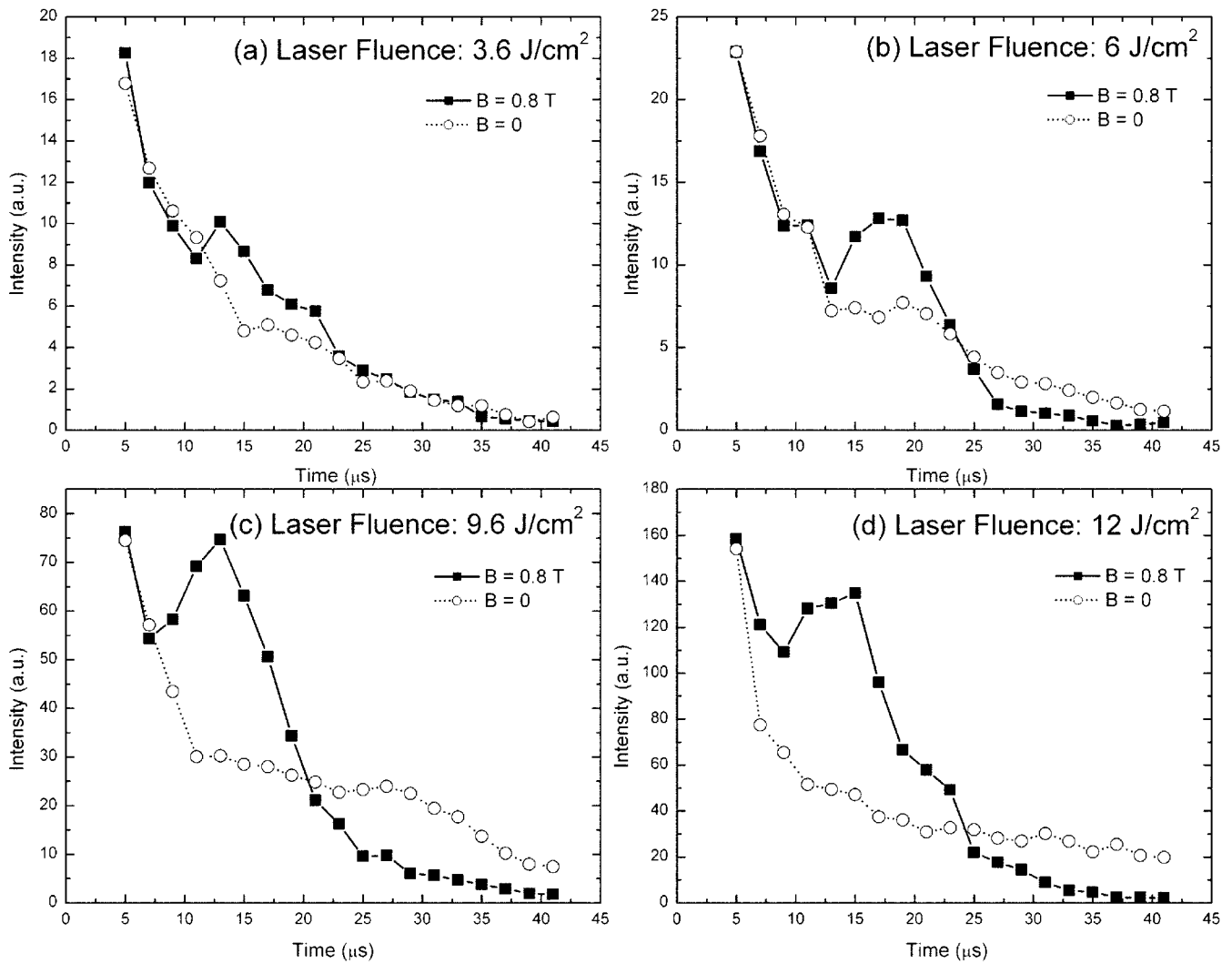


FIG. 7. Optical emission intensity of Al spectral line (394.4 nm, Al I) as a function of delay time at different laser fluences: (a) 3.6, (b) 6, (c) 9.6, and (d) 12 J/cm<sup>2</sup>.

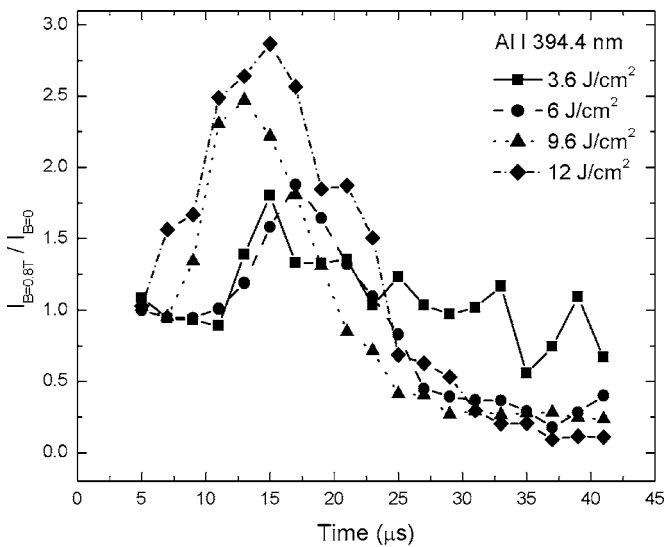


FIG. 8. Comparison of enhancement factors of Al spectral line (394.4 nm, Al I) at different laser fluences.

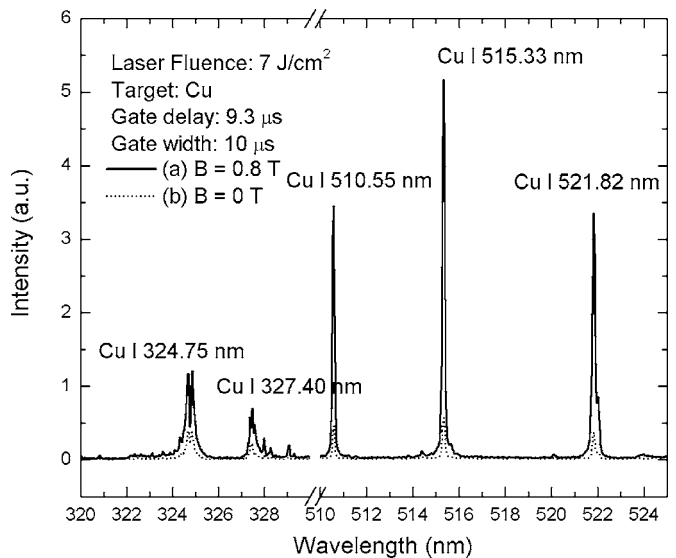


FIG. 9. Time-integrated LIBS of a Cu target at a gate delay of 9.3  $\mu$ s and a gate width of 10  $\mu$ s: (a) with (solid curve) and (b) without magnetic field (dotted curve).

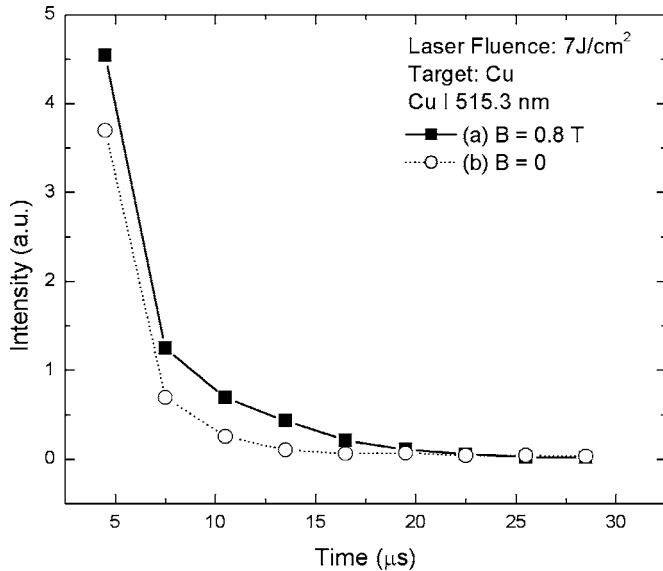


FIG. 10. Emission intensity evolution of Cu spectral lines (515.3 nm, Cu I): (a) with (solid curve) and (b) without magnetic field (dotted curve).

the enhancement of the radiative recombination as a result of increased effective plasma density due to magnetic confinement.

In the magnetically confined LIBS, the enhancement factor is element dependent. The enhancement factors ranged from 2 to 8 under similar experimental conditions. The temporal evolution of the line emissions also varied between different elements. This indicates that the enhancement factors and the dynamics of magnetic confinement depend on the element and excitation properties of samples.

The effect of magnetic field on the LIBS of ferromagnetic materials has also been investigated. Figure 11 shows the LIBS spectra of Co samples measured with (solid curve) and without (dotted curve) the presence of a magnetic field of 0.8 T. The spectrum was obtained with a gate width of 10  $\mu\text{s}$  at a gate delay of 200 ns. The identified emission lines

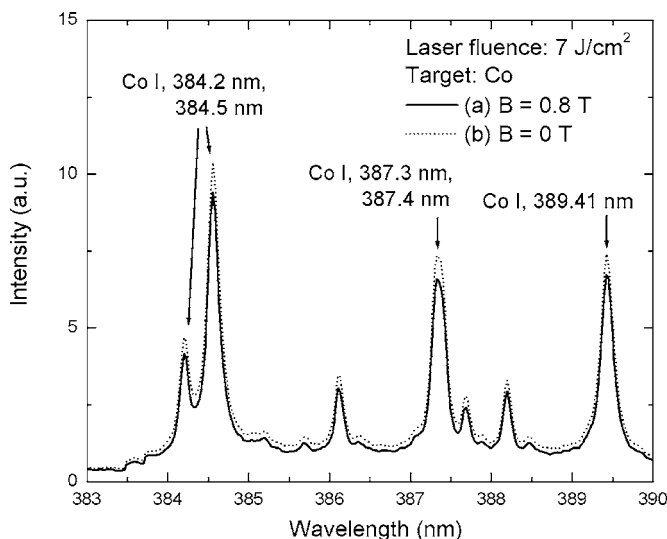


FIG. 11. Time-integrated LIBS of a Co target at a gate delay of 200 ns and a gate width of 10  $\mu\text{s}$ : (a) with (solid curve) and (b) without magnetic field (dotted curve).

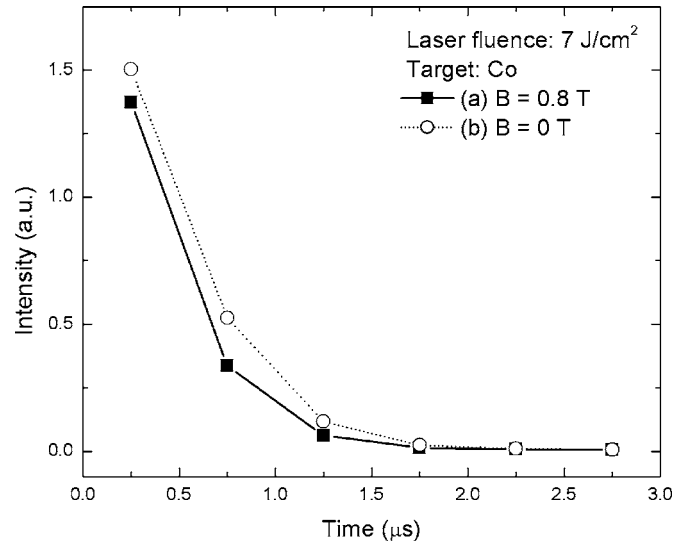


FIG. 12. Emission intensity evolution of Co spectral lines (399.53 nm, Co I): (a) with (solid curve) and (b) without magnetic field (dotted curve).

originate almost from monoatomic cobalt (Co I). It shows that, unlike those nonferromagnetic samples, the optical emission intensity decreased in the presence of a magnetic field. Figure 12 shows the optical emission intensity of the Co atomic line at 399.53 nm as a function of gate delay with (solid curve) and without (dotted curve) a magnetic field of 0.8 T. The emission intensity of Co atomic lines decreases more rapidly than the emission intensity of Al and Cu atomic lines. The time duration of Co atomic emission was nearly 3  $\mu\text{s}$ , while the time durations of Al, Cu, and Mn atomic emissions were nearly 30–50  $\mu\text{s}$ . It is also observed that the optical emission intensity decreased at all gate delay times with the presence of a magnetic field. As compared with Al and Cu, the effective density of laser-induced cobalt plasmas was decreased by the presence of a magnetic field. Therefore, the magnetic force may play an important role in magnetically confined LIBS in addition to the Lorentz force for ferromagnetic materials. Another possible reason for the reduction is that the lifetime of the laser-induced Co plasma is short, and the number density of the excited Co atoms decrease rapidly. As a result, the magnetic confinement effects are not evident.

#### IV. CONCLUSIONS

In summary, enhancement factors of 2 and 6–8 in the optical emission from laser-ablated Al and Cu plasmas were obtained by magnetic confinement using a magnetic field of 0.8 T. The enhancement is probably attributed to the enhanced radiative recombination as a result of increased effective plasma density due to magnetic confinement. Plasma-wall interaction might also occur and contribute to the confinement effect during the expansion of the plasma. Further study about plasma-wall interaction is needed. The temporal profile of spectral lines from Al and Mn impurity were very similar, which is probably due to the collective effect of laser-induced plasmas in magnetic fields. The enhancement factor depends on element and excitation properties of the

samples. In contrast, the optical emission from laser-induced Co plasmas was decreased with the presence of a magnetic field.

## ACKNOWLEDGMENTS

This research was financially supported by U.S. Department of Energy (Nuclear and Radiological National Security Program, National Nuclear Security Administration) through cooperative agreement DE-FC52-04NA25688.

<sup>1</sup>*Laser Induced Plasma and Applications*, edited by L. J. Radziemski and D. A. Cremers (Dekker, New York, 1989).

<sup>2</sup>V. N. Rai, H. Zhang, F. Y. Yueh, J. P. Singh, and A. Kumar, *Appl. Opt.* **42**, 3662 (2003).

<sup>3</sup>J. P. Singh, F. Y. Yueh, H. Zhang, and K. P. Karney, *Recent Res. Dev. Appl. Spectrosc.* **2**, 59 (1999).

<sup>4</sup>M. Corsi, G. Cristoforetti, M. Hidalgo, S. Legnaioli, V. Palleschi, A. Salvetti, E. Tognoni, and C. Vallebona, *Appl. Opt.* **42**, 6133 (2003).

<sup>5</sup>R. A. Multari, L. E. Foster, D. A. Cremers, and M. J. Ferris, *Appl. Spectrosc.* **12**, 1483 (1996).

<sup>6</sup>R. Sattman, V. Sturm, and R. Noll, *J. Phys. D* **28**, 2181 (1995).

<sup>7</sup>D. N. Stratic, K. L. Eland, and S. M. Angel, *Appl. Spectrosc.* **55**, 1297 (2001).

<sup>8</sup>S. S. Harilal, M. S. Tillack, B. O'Shay, C. V. Bindhu, and F. Najmabadi, *Phys. Rev. E* **69**, 026413 (2004).

<sup>9</sup>D. K. Bhadra, *Phys. Fluids* **11**, 234 (1968).

<sup>10</sup>G. Dimonte and L. G. Wiley, *Phys. Rev. Lett.* **67**, 1755 (1991).

<sup>11</sup>A. Neogi and R. K. Thareja, *J. Appl. Phys.* **85**, 1131 (1999).

<sup>12</sup>A. Neogi and R. K. Thareja, *Appl. Phys. B: Lasers Opt.* **72**, 231 (2001).

<sup>13</sup>F. F. Chen, *Introduction to Plasma Physics* (Plenum, New York, 1974).

<sup>14</sup>V. N. Rai, M. Shukla, and H. C. Pant, *Pramana, J. Phys.* **52**, 49 (1999).

<sup>15</sup>V. N. Rai, A. K. Rai, F. Y. Yueh, and J. P. Singh, *Appl. Opt.* **42**, 2085 (2003).

<sup>16</sup>H. C. Pant, V. N. Rai, and M. Shukla, *Phys. Scr., T* **T75**, 104 (1998).